REMARKS

I. Status of Claims

Claims 1-99 were filed with the original application. Claims 90-99 were canceled and new claim 100 advanced in a preliminary amendment. A restriction has resulted in the withdrawal of claims 19-89 (canceled herein), and thus claims 1-18 and 100 are under examination and stand rejected, variously, under 35 U.S.C. §112, first paragraph, 35 U.S.C. §102 and 35 U.S.C. §103. The specific grounds for rejection, and applicants' response thereto, are set out in detail below.

II. Objection

The examiner has objected to the drawings – in particular, claim 6A. Applicants are providing a replacement drawing herewith.

III. Rejection Under 35 U.S.C. §112, First Paragraph

Claims 1-18 and 100 stand rejected under the first paragraph of §112 as allegedly lacking enablement. Claims 12-18 have been canceled without prejudice or disclaimer, and thus applicants' rebuttal is directed to claims 1-11 and 100. With respect to these claims, applicants traverse the rejection.

According to the examiner, the defects in the specification are as follows:

- the claims are broad with respect to treating with a wide range of known kinase inhibitors[1];

[1] In this regard, the rejection is inconsistent with the election of staurosporine as the species of inhibitor. The examiner has not indicated that the species election has been withdrawn, and thus the rejection appears premature.

- there are no working examples of treating with kinase inhibitors nor effective amounts or protocols for such drugs; and
- effective treatment protocols are not described.

So, in essence, the examiner's primary concerns are lack of evidence showing effective treatment. However, it is admitted that kinase inhibitors are indeed well known as are they therapeutic uses. Further, the skill of those in the art is not even mentioned, and applicants submit that it is in fact quite high. Finally, with the cancellation of claims 12-18, the "preventing" aspect of the claims has been dropped, thereby rendering moot any concerns of this nature.

While applicants have admittedly not provided examples of treatment of pathologic cardiac hypertrophy and/or heart failure, what they ***have*** done is unravel the molecular mechanisms by which hypertrophic signaling is initiated and maintained. The fact that they can utilize a known class of drugs – PKD inhibitors – means that they do ***not*** have to undertake ***any*** experimentation on this feature. Rather, one need only determine what doses for what drugs will provide the achieved effect. Given the listed possibilities, including resveratrol, indolocarbazoles, Godecke 6976 (Go6976), staurosporine, K252a, Substance P (SP) analogues including [d-Arg(1),d-Trp(5,7,9), Leu(11)]SP, PKC inhibitor 109203X (GF-1), PKC inhibitor Ro 31-8220, GO 7874, Genistein, the specific Src inhibitors PP-1 and PP-2, chelerythrine, rottlerin, a PKD RNAi molecule, a PKD antisense molecule, a PKD ribozyme molecule or a PKD-binding single-chain antibody, or expression construct that encodes a PKD-binding single-chain antibody, it is not plausible to argue that at least ***some*** of these will enable the claims.

Moreover, applicants have expanded on the work described in the present application in Harrison *et al.* (2006; attached). There, further evidence linking PKD and hypertrophic signaling

is provided, and the use of an inhibitor (siRNA to PKD1) inhibits cardiac hypertrophy in neonatal rat ventricular myocytes (see FIGS. 4A-D) is described.

In sum, applicants submit that the examiner has placed an undue amount of weight on ***one*** fact – the absence of working examples – and ignored positive factors such as the skill in the art and the known pool of proven PKD inhibitors, in coming to a holding of non-enablement. As such, applicants believe that the rejection is improper and request reconsideration and withdrawal thereof.

IV. Rejection Under 35 U.S.C. §102

Claims 1-6, 8-18 and 100 stand rejected over Buchholz *et al.* in view of Bing *et al.* Claims 12-18 have been canceled. With respect to the remaining claims, applicants traverse.

By the examiner's own characterization, the primary reference teaches treating spontaneously hypertensive (SH) rats with staurosporine. However, these rats are not described by the authors as suffering from cardiac hypertrophy. While the *in vivo* methodology section is silent on the age of the animals, two other methods sections indicate that the authors used SH rats aged 15-17 weeks, *i.e.*, less than four months in age. Though Bing *et al.* does indicate that SH rats ***can*** develop cardiac hypertrophy, they do so only during the course of aging (see page 72; right-hand column), with only 59% showing ***pathologic*** heart disease at 19 $\pm$ 2 months. Indeed, persistent hypertension does not even develop until about 2 months of age, followed by "a long period of stable hypertension and ***compensatory*** hypertrophy" (page 72; left-hand column; emphasis added). Thus, the examiner's suggestion that Buchholz *et al.* was ***treating*** hypertrophy misses a key point, namely, that applicants' claims are far more restrictive – they require

treatment of ***pathologic*** (*i.e.*, not compensatory) cardiac hypertrophy or heart failure – neither of which are present in the animals treated by Buchholz *et al.*

Moreover, applicants have amended the claims to recite treatment of a human patient, which clearly is not disclosed in the cited reference. Reconsideration and withdrawal of the rejection is therefore respectfully requested.

V. Rejection Under 35 U.S.C. §103

Claims 1-18 and 100 stand rejected as obvious over Buccholz *et al.*, which is cited as before. In point of fact, this rejection appears to be focused only on claim 7, which is a "combination" claim, where the examiner argues that combining staurosporine with a beta blocker. As such, applicants deem the rejection to be deficient for the reasons already given. However, the following additional comments are provided.

Buchholz *et al.* does not ever mention cardiac hypertrophy. That paper is ***solely*** directed to the issue of treating spontaneous hypertension. So, given that hypertension can ***lead*** to hypertrophy, it may be plausible to argue that Buchholz *et al.* suggests ***preventing*** pathologic cardiac hypertrophy and heart failure using staurosporine, but there is no reasonable basis for believing that one could ***treat*** those disease states with the same drug. This is because there is no direct link in Buchholz *et al.* between kinase inhibition and cardiac hypertrophy and heart failure. Indeed, though aspects of hypertension may well contribute to development of hypertrophy, there was no reason to believe that hypertension could be treated with staurosporine ***once pathologic cardiac hypertrophy existed***, much less that one could also treat the pathologic cardiac hypertrophy and/or the ensuing heart failure, as now claimed. In this regard, applicants urge the examiner not to engage in a hindsight analysis where the facial link between

hypertension and hypertrophy obscures the fact that the mechanism by which staurosporine successfully treated hypertension could well have ***failed*** in the treatment of pathologic cardiac hypertrophy.

Given the lack of understanding of the underlying molecular mechanisms involved in hypertension and hypertrophy at the time of filing, and hence the lack of predictability in extrapolating from treating one to treating the other, a *prima facie* case of obviousness will not stand. Reconsideration and withdrawal of the rejection, in view of applicants' comments above, is respectfully requested.

VI. <u>Conclusion</u>

In light of the foregoing, applicants respectfully submit that all claims are in condition for allowance, and an early notification to that effect is earnestly solicited. Should the examiner have any questions regarding this submission, a telephone call to the undersigned is invited.

Respectfully submitted,

Steven L. Highlander
Reg. No. 37,642
Attorney for Applicants

FULBRIGHT & JAWORSKI L.L.P.
600 Congress Avenue, Suite 2400
Austin, Texas 78701
(512) 536-3184

Date: September 7, 2007

MOLECULAR AND CELLULAR BIOLOGY, May 2006, p. 3875–3888 Vol. 26, No. 10
0270-7306/06/$08.00+0 doi:10.1128/MCB.26.10.3875–3888.2006

Regulation of Cardiac Stress Signaling by Protein Kinase D1

Brooke C. Harrison,[1] Mi-Sung Kim,[2] Eva van Rooij,[2] Craig F. Plato,[1] Philip J. Papst,[1] Rick B. Vega,[2] John A. McAnally,[2] James A. Richardson,[2,3] Rhonda Bassel-Duby,[2] Eric N. Olson,[2]* and Timothy A. McKinsey[1]*

Myogen, Inc., 7575 West 103rd Ave., Westminster, Colorado 80021,[1] and Department of Molecular Biology[2] and Department of Pathology,[3] The University of Texas Southwestern Medical Center at Dallas, 5323 Harry Hines Blvd., Dallas, Texas 75390-9148

Received 29 August 2005/Returned for modification 20 October 2005/Accepted 31 January 2006

In response to pathological stresses such as hypertension or myocardial infarction, the heart undergoes a remodeling process that is associated with myocyte hypertrophy, myocyte death, and fibrosis. Histone deacetylase 5 (HDAC5) is a transcriptional repressor of cardiac remodeling that is subject to phosphorylation-dependent neutralization in response to stress signaling. Recent studies have suggested a role for protein kinase C (PKC) and its downstream effector, protein kinase D1 (PKD1), in the control of HDAC5 phosphorylation. While PKCs are well-documented regulators of cardiac signaling, the function of PKD1 in heart muscle remains unclear. Here, we demonstrate that PKD1 catalytic activity is stimulated in cardiac myocytes by diverse hypertrophic agonists that signal through G protein-coupled receptors (GPCRs) and Rho GTPases. PKD1 activation in cardiomyocytes occurs through PKC-dependent and -independent mechanisms. In vivo, cardiac PKD1 is activated in multiple rodent models of pathological cardiac remodeling. PKD1 activation correlates with phosphorylation-dependent nuclear export of HDAC5, and reduction of endogenous PKD1 expression with small interfering RNA suppresses HDAC5 shuttling and associated cardiomyocyte growth. Conversely, ectopic overexpression of constitutively active PKD1 in mouse heart leads to dilated cardiomyopathy. These findings support a role for PKD1 in the control of pathological remodeling of the heart via its ability to phosphorylate and neutralize HDAC5.

The mammalian heart undergoes a remodeling process when it is subjected to abnormal pathological stressors, such as increased cardiac afterload due to hypertension or loss of functional cardiac tissue resulting from myocardial infarction. The response is characterized by cardiomyocyte death and interstitial fibrosis as well as cardiomyocyte hypertrophy, during which cells increase in size without dividing (7, 26, 35). While cardiac hypertrophy may initially be adaptive, providing benefit by normalizing wall stress, prolonged hypertrophy increases the risk for development of chamber dilation, reduced pump function, and heart failure (13, 34, 45).

Pathological cardiac remodeling is associated with reactivation of the so-called fetal gene program, which encodes proteins involved in contraction, calcium handling, and metabolism (12). Alterations in fetal gene expression have been shown to correlate with loss of cardiac function, and thus investigation has focused on unraveling the transcriptional mechanisms controlling this gene program, with the hope of revealing novel targets that may be amenable to therapeutic manipulation (28).

Recent studies have suggested key roles for histone deacetylases (HDACs) as transcriptional regulators of pathological cardiac remodeling. The acetylation of nucleosomal histones by histone acetyltransferases promotes transcription by relaxing chromatin structure, whereas histone deacetylation by HDACs reverses this process, resulting in transcriptional repression (22). HDACs are divided into three classes based on structural and biochemical characteristics (49). Based on studies with chemical inhibitors, it has been suggested that class I HDACs function as positive regulators of cardiac remodeling (1). In contrast, class II HDAC isoforms 5 and 9 appear to function as negative regulators of cardiac remodeling through association with the myocyte enhancer factor 2 (MEF2) transcription factor and possibly other prohypertrophic transcriptional regulators (28, 52). Indeed, adult mice lacking either HDAC5 or HDAC9 are sensitized to stimuli for pathological cardiac hypertrophy and spontaneously develop cardiomegaly with age (6, 56).

The antihypertrophic action of HDAC5 is overcome by signaling pathways that culminate in nuclear export of this transcriptional repressor (16, 47). Hypertrophic stimuli promote phosphorylation of two conserved serine residues in HDAC5, thereby creating docking sites for the 14-3-3 chaperone protein (14, 21, 30). Binding of 14-3-3 to HDAC5 disrupts its association with MEF2 and triggers its export from the nucleus to the cytoplasm via a CRM1-dependent mechanism, thus freeing MEF2 to activate subordinate genes that govern cardiac hypertrophic growth (16, 29, 30, 47). A signal-resistant form of HDAC5 functions as a potent repressor of cardiac hypertrophy, suggesting that phosphorylation of this histone-modifying enzyme is a requisite step in the process of derepressing genes that drive cardiac growth (47, 56). As such, recent investigation has focused on elucidating the kinase(s) that regulates HDAC5 phosphorylation, with the hypothesis that antagonists of this

* Corresponding author. Mailing address for Timothy A. McKinsey: Myogen, Inc., 7575 West 103rd Ave., Westminster, CO 80021. Phone: (303) 533-1736. Fax: (303) 410-6669. E-mail: timothy.mckinsey@myogen.com. Mailing address for Eric N. Olson: Department of Molecular Biology, The University of Texas Southwestern Medical Center at Dallas, 5323 Harry Hines Blvd., Dallas, TX 75390-9148. Phone: (214) 648-1187. Fax: (214) 648-1196. E-mail: eric.olson@utsouthwestern.edu.

enzyme will block pathological cardiac remodeling and thus provide therapeutic benefit.

We previously demonstrated that cardiac protein kinase C (PKC) signaling stimulates HDAC5 phosphorylation via a downstream effector termed protein kinase D1 (PKD1) (47). Although roles for PKC isozymes as regulators of cardiac signaling are well defined (11, 43, 44), little is known of the function of PKD in the heart. Here, we employ gain- and loss-of-function approaches to assess the role of PKD1 in heart muscle. Our findings demonstrate that PKD1 controls fetal cardiac gene induction and cardiac hypertrophic growth in a manner that correlates with its action on HDAC5. Cardiac PKD1 is activated by multiple stimuli for hypertrophic growth through both PKC-dependent and PKC-independent mechanisms. Importantly, cardiac PKD1 catalytic activity is stimulated in animal models of pathological cardiac hypertrophy, and transgenic mice expressing activated PKD1 in the heart develop dilated cardiomyopathy. These findings demonstrate a novel function for PKD1 in the control of pathological cardiac remodeling via its effects on a chromatin-modifying enzyme.

MATERIALS AND METHODS

Chemical reagents, plasmids, and adenoviral constructs. Phorbol 12-myristate 13-acetate (PMA), phenylephrine (PE), endothelin-1 (ET-1), and isoproterenol (ISO) were obtained from Sigma Chemical Co. Prostaglandin F2α (PGF2α), leukemia inhibitory factor (LIF), tumor necrosis factor (TNF), interleukin-1β (IL-1β), hisindolylmaleimide I (Bis I), and U-73122 were purchased from Calbiochem. Lysophosphatidic acid (LPA) was obtained from Biomol. Agonists were used at the following concentrations: PMA, 50 nM; ET-1, 50 nM; PGF2α, 10 μM; LPA, 10 μM; PE, 20 μM; ISO, 1 μM; LIF, 1,000 U/ml; TNF, 50 ng/ml; and IL-1β, 50 ng/ml. The cDNA encoding wild-type, human PKD1 was a kind gift from A. Toker (Harvard University). For adenovirus production, this cDNA was subcloned into pShuttle-CMV (QBiogen), and adenovirus was generated in HEK293 cells according to the manufacturer's recommendations. Clonal populations of virus were obtained using the agar overlay method and titered with the Adeno-X Rapid Titer kit (Clontech). Adenovirus encoding green fluorescent protein (GFP)-HDAC5 has been described previously (47). The cDNAs encoding GFP-HDAC5 and GFP-HDAC5 (S259/498A) in the pcDNA3.1 expression vector (Invitrogen) have been previously described (47). A vector for constitutively active RhoA (Q63L) was kindly provided by I. Rybkin (University of Texas Southwestern Medical Center).

Cell culture. COS cells were maintained in Dulbecco's minimal essential medium (DMEM) supplemented with 10% fetal bovine serum, 2 mM L-glutamine, and penicillin-streptomycin (DMEM complete). Cells were transiently transfected with Fugene 6 according to the manufacturer's instructions (Roche Molecular Biochemicals). Neonatal rat ventricular myocytes (NRVMs) were prepared from 1- to 2-day-old Sprague-Dawley rats as described previously (1, 32).

Immunoblotting. NRVM whole-cell extracts and in vivo tissue samples homogenized in Tris buffer (50 mM, pH 7.5) containing EDTA (5 mM), Triton X-100 (1%), protease inhibitor cocktail (Complete; Roche), phenylmethylsulfonyl fluoride (1 mM), and phosphatase inhibitors (sodium pyrophosphate [1 mM], sodium fluoride [2 mM], β-glycerol phosphate [10 mM], sodium molybdate [1 mM], and sodium orthovanadate [1 mM]) were used. Lysates were briefly sonicated and cleared by centrifugation. Protein concentrations were determined by bicinchoninic acid assay (Pierce), and 15 μg of total protein was resolved by sodium dodecyl sulfate-polyacrylamide gel electrophoresis (SDS-PAGE) with gradient gels (4 to 20% polyacrylamide; Invitrogen). Proteins were transferred to nitrocellulose membranes (Bio-Rad) and probed with PKD1-specific antibodies according to the manufacturer's instructions (Cell Signaling Technology). Proteins were visualized using an enhanced chemiluminescence system (Pierce).

Indirect immunofluorescence. NRVMs were plated on gelatin-coated 6-well dishes (2.0×10^5 cells/well) in DMEM complete and were transferred 12 h subsequently to serum-free DMEM supplemented with Nutridoma-SP (0.1%; Roche Applied Sciences), which contains albumin, insulin, transferrin, and other defined organic and inorganic compounds the following day. Following experimental treatment, cells were washed twice in phosphate-buffered saline (PBS), fixed with formalin (10%) in PBS, permeabilized and blocked with PBS containing NP-40 (0.1%) and bovine serum albumin (BSA; 3%), and then incubated in the same solution containing primary antibodies specific for either sarcomeric α-actinin (Sigma; 1:200 dilution), total PKD1 (1:1,000 dilution; Cell Signaling Technology), or PKD1 phosphorylated on serine 916 (1:1,000 dilution; Cell Signaling Technology) for either 1 h at room temperature (sarcomeric α-actinin) or overnight at 4°C (PKD1). Cells were washed four times in PBS and incubated in PBS–NP-40–BSA containing either a fluorescein- or CY3-conjugated secondary antibody (1:200 dilution; Jackson Laboratories) for 30 min at room temperature. Cells were washed four times in PBS and then covered with mounting solution (SlowFade; Molecular Probes) and glass coverslips. Proteins were visualized with an inverted fluorescence microscope (Olympus model BH-2) at 40× magnification, and images were captured using a digital camera (Photometrics; Roper Scientific).

Quantification of HDAC5 nuclear export. HDAC5 subcellular localization (nuclear versus cytoplasmic) was quantified as described previously (47). Briefly, cells were plated in the presence of GFP-HDAC5-encoding adenovirus (multiplicity of infection, ~50) on gelatin-coated 96-well dishes (1×10^4 cells/well; Costar) in DMEM complete. The following day, the culture medium was exchanged for serum-free DMEM supplemented with Nutridoma-SP (0.1%). Cells were maintained in serum-free medium for 4 h prior to agonist exposure for 1 h. Cells were fixed with formalin in PBS containing Hoechst dye 33342 (H-3570; Molecular Probes). Relative abundance of GFP-HDAC5 in the nucleus versus the cytoplasm was quantified employing the High Content Imaging System (Cellomics, Inc.), which demarcates nuclei based on Hoechst fluorescence and defines a cytoplasmic ring based on these nuclear dimensions. Values for HDAC5 localization represent averages from a minimum of 400 randomly captured cells per experimental condition.

In vitro kinase assays. Twelve hours postplating, NRVMs (2×10^6) were serum starved for 4 h and subsequently exposed to agonists for 1 h. Following treatment, total protein lysates were prepared as described above for immunoblotting. In vivo tissue samples were homogenized using a Power Gen 1000 homogenizer (Fisher). Total protein (50 to 100 μg) was incubated in buffer (500 μl) containing anti-PKD1 antibody (sc-639; 1:100 dilution; Santa Cruz) overnight at 4°C with rocking. Antibody-protein complexes were captured with protein G Sepharose bead (Amersham) with incubation for 1 h at 4°C. Immunoprecipitates were equilibrated with kinase buffer (20 mM HEPES, pH 7.5, 20 mM $MgCl_2$), and kinase reactions were initiated upon addition of ATP (0.1 mM), 10 μCi [γ-^{32}P]ATP, and 2 μg Syntide-2 substrate (Anaspec). Kinase reactions were carried out at 30°C for 30 min and terminated with either 250 mM EDTA (paper assay) or 2× loading dye (SDS-PAGE). Phospho-Syntide-2 peptide was either resolved by SDS-PAGE and visualized by autoradiography or quantified using p81 Phospho paper circles (VWR) and a Top Count-NXT scintillation counter (Packard).

siRNA studies. Rat PKD1 mRNA sequence was analyzed for potential small interfering RNA (siRNA) target regions using a sequence identification tool (Ambion, Inc.). Potential target sequences were transcribed from oligonucleotide templates using the *Silencer* siRNA Construction kit (Ambion, Inc.). To test for the ability of siRNAs to effectively reduce PKD1 expression, NRVMs were transfected with siRNA (100 nM) using Lipofectamine Plus reagent as specified by the manufacturer (Invitrogen). The rat PKD1-specific siRNA sequences used were the following: #1, 5′-AACCTTCATCACCCTGGTGTT-3′; #2, 5′-AGGC ATTACTGGAGACTGGA-3′; and #3, 5′-AAACTCCATGGAGACATGCTG-3′. A nonspecific siRNA (*Silencer* Negative Control #2; Ambion, Inc.) was used as a negative control. Effects of siRNA on atrial natriuretic factor (ANF) expression, cell volume, and sacromere organization were determined 48 to 72 h posttransfection, as previously described (16).

Reverse transcription-PCR (RT-PCR) analysis of PKD isoform expression. Total RNA from NRVMs was prepared using TRI Reagent (Sigma). First-strand cDNA synthesis was performed using Ready-To-Go You-Prime First-Strand Beads (Amersham) according to manufacturer's instructions. PCRs were programmed with resulting cDNA (30 μl) and PKD isoform-specific primers (PKD1 sense, 5′-GGACTCCTCTGGCGACTACAGC-3′; PKD1 antisense, 5′-GAACG AAGAGAGCGTGAGGCC-3′; PKD2 sense, 5′-GAGGATTTCCAGATCCGT CCGC-3′; PKD2 antisense, 5′-GCTGAAGGCGCAGCGTTTGTGG-3′; PKD3 sense, 5′-TCCAGAGTGTGGATTCTTTGGCATG-3′; PKD3 antisense, 5′-GG TGCTTTGTAAGAATGTACATAGAG-3′).

Animal models of cardiac hypertrophy. The institutional animal care and use committee approved all animal protocols. The spontaneous hypertensive heart failure (SHHF) rat is a well-documented genetic model of hypertension, cardiac hypertrophy, and heart failure (36). SHHF males and age-matched Wistar-Furth control animals were sacrificed at 15 to 20 months of age. Thoracic aortic banding was performed as described previously using male SHHF rats 3 months of age (57). For the acute norepinephrine model, male Sprague-Dawley rats were injected subcutaneously with either vehicle control (1 mg/ml ascorbic acid in

sterile distilled H_2O) or norepinephrine (dissolved in vehicle sufficient to administer 10 mg norepinephrine/kg of body weight).

Transgenic mouse production. A cDNA encoding constitutively active human PKD1 was kindly provided by A. Toker (Harvard University). This construct encodes PKD1 containing glutamic acid residues in place of the PKC phosphorylation sites at serines 744 and 748. The cDNA was subcloned into a cardiac-specific expression plasmid containing the α-myosin heavy chain promoter and human GH poly(A)$^+$ signal (15). DNA isolation and oocyte injections were performed as described previously by using oocytes derived from B6C3 mice (32). Genomic DNA was isolated from mouse tail biopsies and analyzed by PCR using primers specific for the human GH poly(A)$^+$ signal.

Transthoracic echocardiography. Two-dimensional echocardiography was performed in conscious mice using the fully digital Vingmed System (GE Vingmed Ultrasound, Horten, Norway) and a 11.5-MHz linear array transducer. Cine loops and still images were digitally stored for subsequent analysis using the EchoPac software (GE Vingmed Ultrasound). Two-dimensional short-axis views of the left ventricle (LV) at the level of the tip of the papillary muscle were recorded with a typical frame rate of 263/s. LV parameters and heart rates were obtained from M-mode interrogation in a short-axis view. M-mode tracings were used to measure anterior and posterior wall thicknesses at end diastole and end systole, and LV internal diameter (LVID) was measured as the largest anteroposterior diameter in either diastole (LVIDd) or systole (LVIDs). The data were analyzed by a single observer blinded to mouse genotype. LV fractional shortening (FS) was calculated according to the following formula: FS (%) = [(LVIDd − LVIDs)/LVIDd] × 100.

RESULTS

Differential responsiveness of cardiac PKD1 to extracellular agonists. PKD1 contains two cysteine-rich domains (CRDs) that bind diacylglycerol (DAG), a pleckstrin homology (PH) autoinhibitory domain, and a carboxy-terminal, serine/threonine kinase catalytic domain (Fig. 1A). PKC-mediated phosphorylation of serines 744 and 748 (designated S744/748) in the activation loop of PKD1 results in stimulation of PKD1 catalytic activity (8, 50–52, 58), as evidenced by autophosphorylation of serine 916 (S916) (27). To assess the responsiveness of PKD1 to various growth-promoting agonists in cardiac myocytes, immunoblotting studies were performed with antibodies that recognize PKD1 when phosphorylated at S744/748 or S916. As shown previously, PKD1 phosphorylation was potently elevated in cultured neonatal rat ventricular myocytes (NRVMs) following 1 h of stimulation with the cell-permeable PKC activator PMA (18). Similarly, agonists that stimulate the following GPCRs enhanced PKD1 phosphorylation: the ET receptor (ET-R), the PGF2α receptor, the LPA receptor, and the α_1-adrenergic receptor (α_1-AR). In contrast, stimulation of the β-adrenergic receptor (β-AR), which is also a GPCR, or the LIF, TNF-α, or IL-1β cytokine receptor did not result in observable changes in PKD1 phosphorylation state (Fig. 1B).

To confirm that phosphorylation of PKD1 correlates with increased activity of the kinase, immunoprecipitation and in vitro kinase assays were performed with extracts from control and agonist-stimulated NRVMs. Consistent with the immunoblotting results, endogenous PKD1 from cells treated with ET-1, PE, or PMA exhibited an increased ability to phosphorylate a substrate peptide (Syntide-2) in vitro compared to PKD1 from untreated cells (Fig. 1C). Kinase activity was undetectable when samples were immunoprecipitated with control antibody specific for IκB kinase-2 (IKK-2).

To determine the kinetics of PKD1 activation in cardiac myocytes, NRVMs were stimulated with the α_1-AR agonist PE over a time course of 1 to 24 h. As shown in Fig. 1D, cardiac PKD1 was activated within 15 min of PE exposure, and activation was sustained for at least one day.

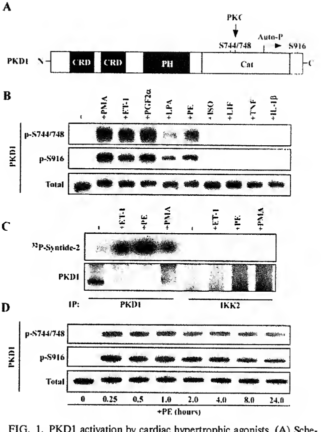

FIG. 1. PKD1 activation by cardiac hypertrophic agonists. (A) Schematic representation of PKD1 structure showing the relative locations of known regulatory regions, including the two N-terminal, cysteine-rich domains (CRD), the pleckstrin homology (PH) domain, and the catalytic domain (Cat). Located within the catalytic domain are two activation-loop serine residues (S744/748) known to be targets for PKC-mediated phosphorylation. Upon phosphorylation by PKC, PKD1 undergoes autophosphorylation (Auto-P) on serine 916 (S916). (B) NRVMs were left untreated (−) or were stimulated for 1 h with the indicated agonists, as described in Materials and Methods. Immunoblotting experiments revealed agonist-dependent phosphorylation of both activation loop (S744/748) and autophosphorylation (S916) residues of PKD1. (C) Immunoprecipitation and in vitro kinase experiments using anti-PKD1 antibodies revealed increased Syntide-2 substrate phosphorylation by PKD1 derived from NRVMs stimulated with ET-1, PMA, or PE. Control pull-down experiments using an IKK-2-specific antibody showed no detectable Syntide-2 phosphorylation. Parallel immunoprecipitates were subjected to immunoblotting with anti-PKD1 antibodies (lower panels). Smearing is due to recognition of immunoprecipitating antibody by secondary immunoblotting antibody. (D) NRVMs were left untreated (0) or were stimulated with PE for the indicated times. Protein lysates were prepared and immunoblotted with the indicated antibodies.

Coordinate activation of cardiac PKD1 and HDAC5 nuclear export. Prior studies have shown that PKD1 is capable of functioning as an HDAC5 nuclear export kinase (47). However, the extent to which PKD1 controls agonist-mediated nucleocytoplasmic shuttling of HDAC5 in cardiac myocytes has not been investigated. To begin to address this issue, we monitored the subcellular distribution of a GFP-HDAC5 fusion protein in NRVMs treated with the panel of agonists described above. GFP-HDAC5 was largely confined to the nuclei of unstimulated NRVMs (Fig. 2A). However, treatment of the cells with agonists that stimulate PKD1 (PMA, ET-1, PGF2α,

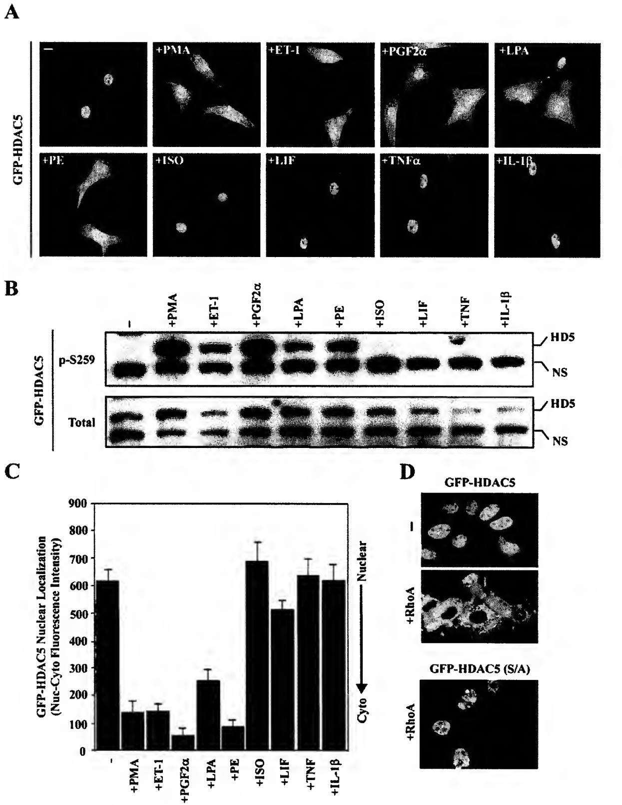

FIG. 2. PKD1 activation correlates with nuclear export of HDAC5. (A) NRVMs were infected with adenovirus encoding GFP-HDAC5 and stimulated with the indicated agonists for 1 h. Cells were fixed and stained with Hoechst dye to reveal nuclei (blue). Only those agonists that increased PKD1 phosphorylation (PMA, ET-1, PGF2α, LPA, and PE) resulted in nuclear export of GFP-HDAC5. Hoechst staining is only shown in cases where HDAC5 underwent nuclear export. (B) NRVMs were infected with adenovirus encoding GFP-HDAC5 and treated as described for panel A. Protein lysates were subjected to immunoblotting with antibody that recognizes HDAC5 when phosphorylated on S259 (upper panel)

LPA, and PE) promoted rapid nuclear export of HDAC5. In contrast, those agonists that failed to alter PKD1 phosphorylation status (ISO, LIF, TNF-α, and IL-1β) had no effect on the subcellular distribution of HDAC5. These findings were confirmed by employing a quantitative nuclear export assay (Fig. 2C).

PKD signaling triggers phosphorylation of HDAC5 on two serine residues, S259 and S498 (47). To determine whether agonist-dependent nuclear export of HDAC5 correlates with phosphorylation of these sites, immunoblotting studies were performed with an antibody specific for HDAC5 when phosphorylated on S259. As shown in Fig. 2B, HDAC5 phosphorylation was triggered only by agonists that also stimulated PKD activation (Fig. 1B) and HDAC5 nuclear export (Fig. 2A).

Rho family small GTPases are important mediators of GPCR signaling in cardiac myocytes and have been shown to stimulate PKD1 activity (19, 55). As such, we also investigated the ability of Rho GTPases to stimulate nuclear export of HDAC5. Overexpression of constitutively active RhoA in COS cells resulted in nuclear export of HDAC5 that correlated with PKD1 activation (Fig. 2D and data not shown). An HDAC5 mutant harboring alanines in place of the phosphoacceptor serines at positions 259 and 498 (S259/498A) was resistant to RhoA signaling. Of note, the RhoA-related factors Rac and cdc42 did not appear to affect HDAC5 localization (data not shown).

siRNA-mediated knockdown of PKD1 blunts agonist-mediated nuclear export of HDAC5. To further examine the role of PKD1 signaling in the control of HDAC5 nuclear export, we developed an siRNA method to specifically suppress endogenous PKD1 expression in NRVMs. Transfection of NRVMs with a PKD1-specific siRNA resulted in marked, time-dependent downregulation of PKD1 protein expression (Fig. 3A). In contrast, a nonspecific control siRNA had no effect on PKD1 levels. RT-PCR analysis revealed that the PKD1 siRNA did not alter expression of PKD2 or PKD3 mRNA transcripts (Fig. 3B).

With a specific tool for reducing PKD1 expression in hand, we next assessed the effects of PKD1 downregulation on agonist-dependent nuclear export of HDAC5. Suppression of PKD1 expression resulted in a ~50% reduction in HDAC5 nuclear export mediated by agonists of the ET-R (ET-1) or the α_1-AR (PE) (Fig. 3C and D; data not shown). In contrast, nonspecific control siRNA had no discernible effect on HDAC5 nuclear export. Taken together, these results suggest a role for PKD1 signaling in the control of HDAC5 nuclear export in cardiac myocytes.

Downregulation of PKD1 expression suppresses cardiac hypertrophy. In light of the ability of PKD1 siRNA to suppress nuclear export of HDAC5, we examined the effects of reducing PKD1 expression on agonist-dependent cardiac hypertrophy. Cardiomyocyte hypertrophy is associated with increased cell size due to enhanced protein synthesis, reactivation of fetal cardiac genes, including the gene encoding secreted atrial natriuretic factor (ANF), and increased assembly and organization of sarcomeres. For these studies, we employed three different PKD1-specific siRNA sequences, each of which potently reduced endogenous PKD1 protein in NRVMs (Fig. 4A) (siRNA #1 is the same as that used for the experiments shown in Fig. 3). Coulter Counter analysis of NRVM cell volume revealed a 67% increase in cell size in control cells treated with PE, while PKD1 siRNA-transfected cells increased in size by only ~17% upon PE treatment (Fig. 4B). Each of the PKD1 siRNAs resulted in similar reductions in cell size. Since each siRNA targets a distinct region of the PKD1 mRNA transcript, the results suggest that the phenotype was dependent on reduced PKD1 expression and not due to an off-target effect. Suppression of PKD1 expression also significantly reduced agonist-mediated induction of ANF secretion into culture supernatants (Fig. 4C).

In NRVMs expressing control siRNA, treatment with PE led to parallel assembly of highly ordered sarcomeres. In contrast, cells transfected with siRNA directed against PKD1 were partially resistant to the sarcomere-altering effects of PE (Fig. 4D). Using adenylate kinase release into the culture medium as a marker of cellular toxicity, we found no evidence of siRNA-induced cell death (data not shown). These results suggest that PKD1 signaling contributes to agonist-dependent cardiomyocyte hypertrophy.

PKC-dependent and -independent activation of PKD1 in cardiomyocytes. Prior studies have demonstrated that PKD1 activation is dependent on PKC signaling (40), and results shown in Fig. 1B suggest a similar mechanism for controlling cardiac PKD1 activity. As such, we hypothesized that the potent, broad-spectrum PKC inhibitor Bis I would block cardiac PKD1 activation in response to multiple hypertrophic agonists. Indeed, Bis I completely blocked phosphorylation of PKD1 activation loop site S744/748 in response to either PE or ET-1 (Fig. 5A). However, although Bis I inhibited PE-mediated autophosphorylation of PKD1 at S916, the compound had no effect on S916 phosphorylation in response to ET-1. Similar results were obtained with independent PKC inhibitors, including Gö-6983 (data not shown).

Prior studies have indicated that the subcellular distribution of PKD1 is altered in response to agonists (38). To extend the above findings, indirect immunofluorescence studies were performed to assess the localization of PKD1 in cardiac myocytes. As shown in Fig. 5B, diffuse cytoplasmic staining of PKD1 was detected in unstimulated cardiomyocytes and, consistent with the immunoblotting studies in Fig. 5A, this pool of PKD1 did not appear to be autophosphorylated on S916. Both PE and ET-1 stimulated phosphorylation of S916, with resulting redis-

or antibody to total HDAC5 (lower panel). NS, nonspecific. (C) Nuclear versus cytoplasmic distribution of GFP-HDAC5 was quantified with the Cellomics high-content imaging system, as described in Materials and Methods. Mean nuclear minus cytoplasmic fluorescence intensity was determined for at least 50 cells/well with 8 wells per condition. Higher values represent a greater abundance of GFP-HDAC5 in the nucleus. Values represent means ± standard deviations. Nuc, nuclear; cyto, cytoplasmic. (D) COS cells were cotransfected with either empty expression vector or a plasmid encoding constitutively active RhoA (0.5 μg/well) and a GFP-HDAC5 expression construct (1.0 μg/well). Overexpression of RhoA in COS cells stimulated nuclear export of GFP-HDAC5. An HDAC5 mutant harboring alanines in place of the PKD1 target serines (GFP-HDAC5 [S/A]) was resistant to RhoA-mediated nuclear export.

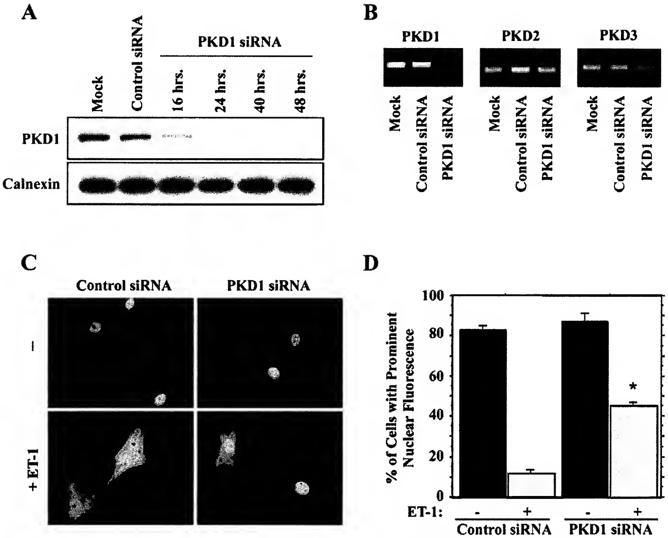

FIG. 3. siRNA-mediated knockdown of PKD1 inhibits agonist-dependent nuclear export of GFP-HDAC5. (A) NRVMs were transfected with siRNA (100 nM) the day after plating. Cells were harvested at the indicated times posttransfection, and PKD1 levels were determined by immunoblotting. Cells transfected with PKD1-specific siRNA showed a time-dependent reduction in PKD1 protein expression. (B) RNA was prepared from NRVMs 48 h posttransfection with control or PKD1-directed siRNA. RT-PCR analysis of mRNA transcripts revealed PKD1-specific gene silencing with no effect on expression of PKD2 or PKD3. (C) NRVMs were transfected with control or PKD1-directed siRNA. One day following transfection, cells were infected with adenovirus encoding GFP-HDAC5. After 24 h of adenovirus infection, cells were stimulated for 1 h with ET-1 (50 nM), fixed, and imaged. (D) Manual quantification of GFP-HDAC5 cellular localization revealed a significant reduction in the ability of ET-1 to trigger nuclear export of GFP-HDAC5 in cells with reduced PKD1 expression. Cells were visualized and GFP-HDAC5 localization was classified as either prominent nuclear, cytosolic, or pan-cellular. Two independent investigators performed this analysis and obtained similar results. Values represent combined means ± standard errors of the means from three duplicate experiments. n = 100 cells per condition, per experiment.

tribution of PKD1 to the nucleus and the perinuclear region of the cardiomyocyte. Bis I effectively blocked PKD1 activation and redistribution in response to PE but had no effect on the responses of PKD1 to ET-1.

Phospholipase C (PLC) lies downstream of the α_1-AR and ET-R and contributes to PKC activation by catalyzing the formation of DAG. Experiments were performed to address the role of PLC in the control of PKD1 and HDAC5 in cardiac myocytes. The PLC inhibitor U-73122 dose dependently suppressed cardiac PKD1 activation in response to ET-1 and PE (Fig. 5C and data not shown) and potently repressed nuclear export of HDAC5 (Fig. 5D). These findings suggest a role for PLC in both PKC-dependent and -independent activation of PKD1.

PKD1 is activated during pathological cardiac hypertrophy in vivo. In order to address the possible role of PKD1 signaling in the control of pathological cardiac hypertrophy in vivo, we analyzed the phosphorylation state of PKD1 in left ventricular tissue from rodent models of cardiac hypertrophy and heart failure. Immunoblotting experiments revealed that acute and chronic infusion of norepinephrine, which triggers both α- and β-ARs, resulted in a marked increase in PKD1 phosphorylation by PKC at serines 744 and 748 and autophosphorylation at S916 (Fig. 6A) (data not shown). Consistent with the in vitro

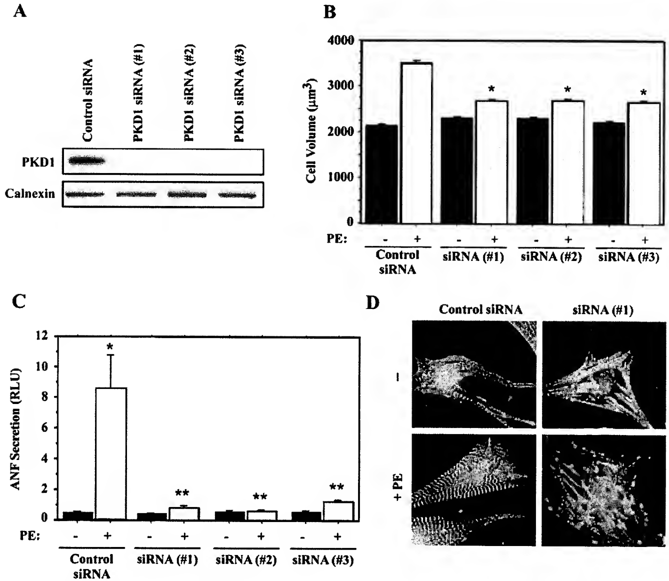

FIG. 4. siRNA-mediated knockdown of PKD1 inhibits cardiac hypertrophy. (A) NRVMs were transfected with control-directed siRNA or three distinct PKD1-directed siRNAs (#1 to #3; 100 nM) for 3 h. Cells were cultured in serum-free medium for 48 h prior to preparation of protein lysates. Endogenous levels of PKD1 protein were detected by immunoblotting. Blots were reprobed with anti-calnexin antibody to control for protein loading. (B) NRVMs were transiently transfected with the indicated siRNAs and either left untreated or stimulated with PE (20 μM) for an additional 48 h. Cell volumes were measured using a Coulter Counter. Values represent mean cubic micrometers (± standard errors of the means) for 60,000 cells from 6 independent culture wells. *, $P < 0.0001$ versus values for PE-treated control cells. (C) ANF abundance in culture supernatants from panel B was quantified by enzyme-linked immunosorbent assay and is represented as mean nanograms/milliliter (± standard deviations) from 6 independent culture wells per experimental condition. *, $P < 0.0001$ versus values for PE-treated control cells. (D) NRVMs were transfected and stimulated with PE as described for panel B. After 48 h of treatment, cells were fixed and sarcomeres were visualized by indirect immunofluorescence with sarcomeric α-actinin-specific antibodies. Reduction of PKD1 expression resulted in reduced sarcomere assembly and organization in agonist-treated cells.

results (Fig. 1B), selective stimulation of β-ARs with ISO did not result in activation of cardiac PKD1 in vivo (data not shown). PKD1 phosphorylation was also consistently elevated in hearts of spontaneously hypertensive heart failure (SHHF) rats compared to age-matched controls (Fig. 6B). Immunoprecipitation and in vitro kinase experiments confirmed that the increase in cardiac PKD1 phosphorylation state correlated with elevated kinase catalytic activity (Fig. 6C). In addition, when SHHF rat hearts were subjected to pressure overload due to thoracic aortic banding, we observed exaggerated PKD1 activation that correlated with enhanced cardiac hypertrophy (Fig. 6D). Of note, the apparent difference in PKD1 phosphorylation state in Fig. 6B (SHHF) and D (sham) is due to differences in film exposure time. Together, these findings are consistent with a role for PKD1 signaling in the control of pathological cardiac growth.

PKD1 overexpression stimulates pathological cardiac hypertrophy in vivo. To further explore the role of PKD1 in the

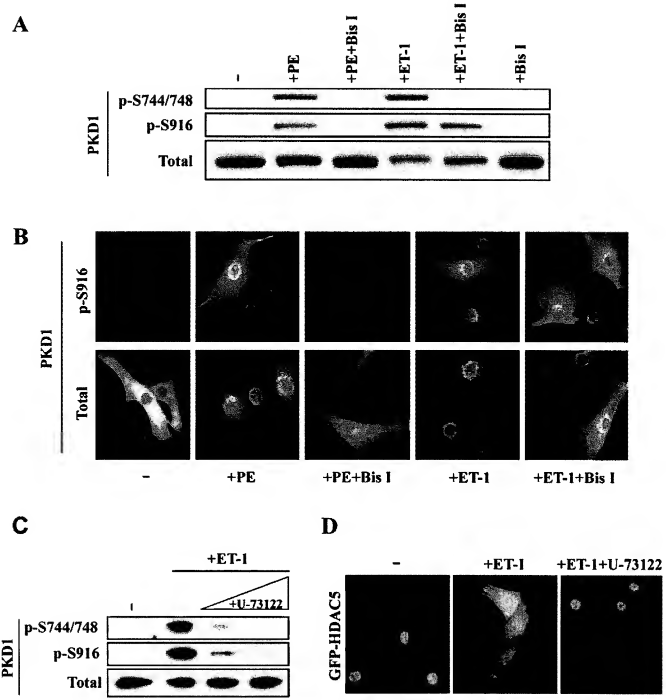

FIG. 5. PKC-dependent and -independent activation of PKD1. (A) NRVMs were left unstimulated (−) or were treated for 1 h with PE (20 μM) or ET-1 (50 nM) in the absence or presence of the general PKC inhibitor Bis I (10 μM). Immunoblotting experiments of protein lysates revealed agonist-dependent phosphorylation of both activation loop (S744/748) and autophosphorylation (S916) sites in PKD1. (B) NRVMs were infected with adenovirus encoding wild-type PKD1 (multiplicity of infection, 20). Cells were left unstimulated (−) or were treated with PE (20 μM) or ET-1 (50 nM) for 1 h in the absence or presence of Bis I (10 μM). Cells were fixed, and the subcellular distribution of PKD1 was determined by immunofluorescence with antibodies against PKD1 phosphorylated at S916 (upper panels) or total PKD1 (lower panels). (C) Immunoblot analysis of PKD1 phosphorylation at S744/748 and S916 in NRVMs stimulated for 1 h with ET-1 (50 nM) in the absence or presence of the phospholipase C (PLC) inhibitor U-73122 (0.5 μM or 1.0 μM). (D) NRVMs were infected with adenovirus encoding GFP-HDAC5. Cells were stimulated with ET-1 (50 nM) in the absence or presence of U-73122 (1 μM). PLC inhibition completely blocked ET-1-mediated nuclear export of HDAC5.

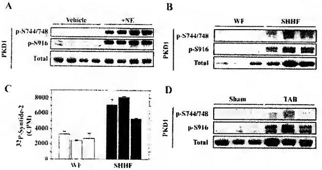

FIG. 6. PKD is activated during pathological cardiac hypertrophy in vivo. (A) Left ventricular protein extracts were prepared from 5-month-old Sprague-Dawley rats infused with norepinephrine (NE; 10 mg/kg) or vehicle control (saline) for 1 h. Levels of total PKD1, PKD1 phosphorylated by PKC on S744/748, and PKD1 autophosphorylated on S916 were determined by immunoblotting. (B) PKD1 activation state was analyzed in left ventricular tissues from 15- to 20-month-old spontaneously hypertensive, heart failure rats (SHHF) or age-matched Wistar-Furth (WF) control rats, as described for panel A. (C) Left ventricular protein from three independent WF or SHHF rats was immunoprecipitated with anti-PKD1 antibody, and immunoprecipitates were incorporated into in vitro kinase assays with Syntide-2 substrate and [^{32}P]ATP. Increased phosphorylation of S916 correlates in elevated PKD1 kinase activity. (D) Three-month-old SHHF rats were subjected to thoracic aortic banding, as described in Materials and Methods. Thoracic aortic banding (TAB) exaggerates PKD1 activation in SHHF rat hearts. The apparent difference in PKD1 phosphorylation state in panels B (SHHF) and D (sham) is due to differences in film exposure time.

control of cardiac hypertrophy, we generated transgenic mice that express a constitutively active form of PKD1 in the heart under control of the α-MyHC promoter. This PKD1 mutant harbors negatively charged aspartic acid residues at positions 744 and 748, thereby bypassing the need for PKC-mediated phosphorylation of these activation loop sites. As shown in Fig. 7A, PKD1 activity was dramatically upregulated in hearts of these mice. Cardiac PKD1 activation resulted in ventricular chamber dilation, wall thinning, and enlargement of atria (Fig. 7B). Thrombi were often observed in explanted transgenic hearts. PKD1 activation in the heart was associated with myocyte disarray, nonuniform myocyte hypertrophy, and increased interstitial space. Of note, only minimal fibrosis was observed in PKD1 transgenic hearts (data not shown).

Expression of fetal cardiac genes, including those for ANF, brain natriuretic peptide (BNP), α-skeletal actin (α-Sk-Ac), and β-myosin heavy chain (β-MyHC), was dramatically elevated in hearts of PKD1 transgenic animals (Fig. 7C). This level of fetal gene activation surpassed that seen in mice expressing active calcineurin in the heart, which develop profound cardiomegaly (Fig. 7C) (32).

To further examine the impact of PKD1 activation on cardiac morphology and function, PKD1 transgenic animals and wild-type littermates were subjected to serial analysis by two-dimensional and M-mode echocardiography at 4, 6, 8, and 12 weeks of age. Representative images of M-mode recordings are shown in Fig. 8A. As early as 4 weeks of age, cardiac overexpression of PKD1 induced an increase in left ventricular diameter and thinning of both the anterior and posterior walls compared to those of wild-type littermates (Fig. 8B). The geometric changes in the heart progressed in a time-dependent manner and were accompanied by deterioration in cardiac function, as indicated by a decreased fractional shortening (Fig. 8B and Table 1). Together, these data demonstrate that chronic PKD1 activation in the heart triggers pathological cardiac remodeling.

DISCUSSION

Myocardial hypertrophy in response to increased cardiac afterload or decreased viable cardiac tissue is an important predictor of mortality due to heart failure, which is a major cause of death in the Western world (10, 13, 45). The data presented here support a role for the serine/threonine kinase PKD1 in the control of stress-induced cardiac hypertrophy. The progrowth effects of PKD1 appear to be mediated, at least in part, by phosphorylation of HDAC5. PKD1-mediated phosphorylation triggers shuttling of HDAC5 from the nucleus to the cytoplasm, where it is no longer capable of repressing expression of genes that drive myocyte growth. The results of this study suggest that small molecules designed to selectively antagonize PKD1 activity may provide a therapeutic benefit for patients with cardiac disease.

Three PKD isoforms. Our studies have focused on PKD1. However, it should be noted that PKD2 and PKD3 are expressed in cardiac myocytes (see Fig. 3B) and that these PKD isoforms are capable of phosphorylating HDAC5 in vitro (K. Huyhn and T. A. McKinsey, unpublished results). As such, we cannot rule out the possibility that PKD2 and/or PKD3 functions redundantly or in concert with PKD1 to control HDAC5 phosphorylation and cardiac hypertrophy. In this regard, suppression of PKD1 expression with siRNA resulted in a ~50% reduction in the degree of agonist-dependent nuclear export of HDAC5 (Fig. 3). Thus, the incomplete repression of this process by PKD1 siRNA may be a reflection of the action of PKD2 and/or PKD3. Alternatively, the results may be a consequence of incomplete knockdown of PKD1 expression or the involvement of other HDAC kinases, such as Ca^{2+}/calmodulin-dependent kinase.

Sufficiency of PKD1 signaling for induction of cardiac hypertrophy? The fact that siRNA-mediated reduction of PKD1 expression in NRVMs blunts cardiac hypertrophy suggests that signaling via this kinase is necessary for stress-mediated cardiomyocyte growth (Fig. 4). In addition, ectopic expression of constitutively active PKD1 in mouse heart is sufficient to trigger pathological cardiac remodeling (Fig. 7 and 8). However, we note that adenovirus-mediated overexpression of active PKD1 in NRVMs does not stimulate hypertrophic growth of the cells (data not shown), leading to the conclusion that PKD1 signaling is only sufficient to stimulate cardiac hypertrophy in the context of the whole animal. The reason for this discrepancy remains unknown, but it may reflect a dependence on crosstalk between myocytes and other cell populations within the heart, such as fibroblasts. Alternatively, PKD1-mediated hypertrophy may require tonic stimulation of parallel or interconnected signaling pathways.

PKC-dependent and -independent activation of cardiac PKD1. Numerous studies have demonstrated that PKC-mediated phosphorylation of S744/748 in the catalytic domain of PKD1 is a key mechanism for activation of the kinase (50–52,

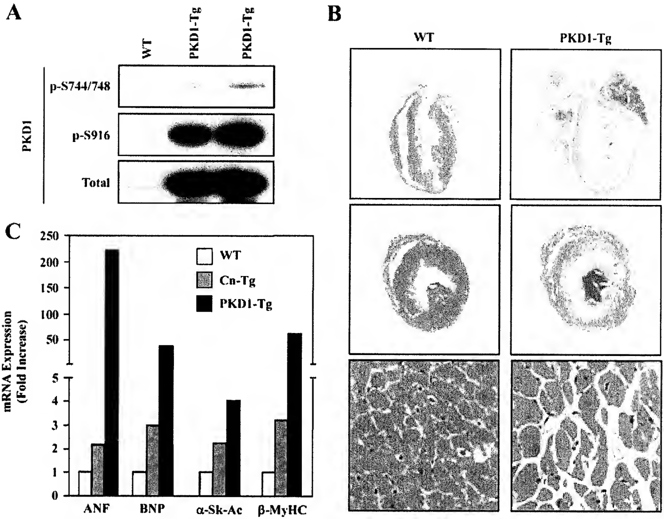

FIG. 7. Cardiac-specific overexpression of active PKD1 triggers pathological hypertrophy in mice. (A) PKD1 phosphorylation state in wild-type mice (WT) and two independent α-MyHC-PKD1 transgenic mouse lines (PKD1-Tg) was measured by immunoblotting with total heart protein lysates. (B) Histological sections revealed gross enlargement of ventricles and atria in 3-month-old PKD-Tg mice compared to WT littermates (upper panels, 1-month-old animals; middle panels, 3-month-old animals). Wall thinning and chamber dilation in PKD1-Tg mice was accompanied by myocyte disarray, sporadic myocyte hypertrophy, and increased interstitial space (lower panels, 3-month-old animals). (C) Total RNA was prepared from 10-week-old PKD1-Tg transgenic mice, WT littermates, or mice expressing constitutively active calcineurin in the heart (Cn-Tg). Expression of fetal cardiac genes for ANF, BNP, α-skeletal actin (α-Sk-Ac), and β-MyHC was assessed by quantitative RT-PCR. The bar graph indicates relative mRNA levels normalized by GAPDH. The relative level of mRNA in the wild type is assigned a value of 1.

58). In cardiac myocytes, we also observed agonist-dependent phosphorylation of S744/748 that paralleled activation of PKD1 (Fig. 1B). In the case of α_1-AR signaling, PKC-dependent phosphorylation of these sites appeared to be required for PKD1 activation, since the PKC inhibitor Bis I blocked both phosphorylation of S744/748 and autophosphorylation of S916 (Fig. 5A). These findings are in line with those of Haworth et al. (18). Conversely, while ET-R signaling also stimulated phosphorylation of S744/748, blockade of this posttranslational modification with Bis I did not inhibit autophosphorylation at S916, suggesting that ET-1-mediated PKD1 activation occurs in a PKC-independent manner (see Fig. 8). A model summarizing our results is shown (Fig. 9).

PKC-independent mechanisms for controlling PKD1 activity in intact cells have been described and include Abl kinase-mediated phosphorylation of tyrosine 463 in the PH domain of PKD1 as well as direct binding of DAG to the cysteine-rich domains of PKD1 (41, 42, 53). However, these modifications do not appear to be sufficient to stimulate PKD1 activity but rather serve to enhance PKC-mediated activation of the kinase. Apart from our findings in cardiac myocytes, the only other report of PKD1 activation in the absence of S744/748 phosphorylation was in osteoblastic cells exposed to bone morphogenetic protein (23).

The mechanism whereby ET-R signaling triggers PKC-independent activation of PKD1 in cardiac myocytes is unknown. It should be noted that this response still requires PLC signaling (Fig. 5C), and thus could involve direct binding of DAG to the CRD of PKD1. Alternatively, PLC may stimulate tyrosine

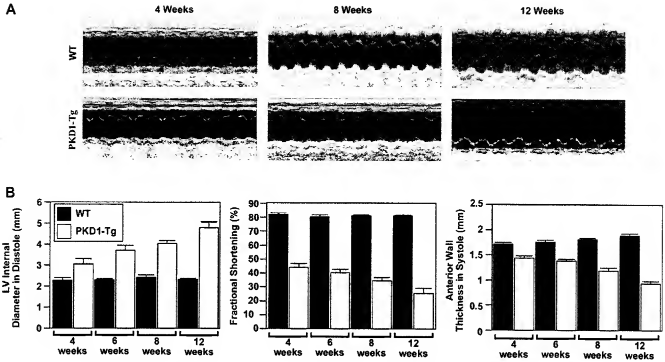

FIG. 8. Impaired cardiac function in PKD1 transgenic mice. (A) Representative M-mode images of wild-type (WT) or PKD1 transgenic (PKD1-Tg) mice at 4, 8, and 12 weeks of age. Data demonstrate initial LV dilation and wall thinning in PKD1 transgenic animals, which progresses in time and results in a decrease in cardiac function. (B) Bar graph representation of left ventricular internal diameter in diastole as well as fractional shortening and anterior wall thickness in systole. Values represent averages from the following animals (*n*): WT, 4 weeks old (4); WT, 6 weeks old (4); WT, 8 weeks old (3); WT, 12 weeks old (3); PKD1-Tg, 4 weeks old (8); PKD1-Tg, 6 weeks old (6); PKD1-Tg, 8 weeks old (6); and PKD1-Tg, 12 weeks old (3). PKD1 activation attenuates cardiac function and alters LV morphology in an age-dependent manner.

and/or serine/threonine kinases that target PKD1 distally to S744/748 (Fig. 9).

RhoA-dependent nuclear export of HDAC5. We provide evidence that signaling via Rho GTPases triggers phosphorylation-dependent nuclear export of HDAC5. Rho family members have long been implicated in the control of pathological cardiac hypertrophy, and they were recently identified as the targets of statins that enable these drugs to exert beneficial effects on the heart (24). However, the downstream effectors of Rho GTPases that mediate cardiomyocyte growth have remained poorly defined. Our data suggest that RhoA-mediated cardiac hypertrophy is governed, in part, through activation of PKD1, which leads to phosphorylation-dependent neutralization of HDAC5. RhoA-stimulated nuclear export of HDAC5 is blocked by Bis I (data not shown), which is consistent with a prior study revealing a role for PKC in the activation of PKD1 by this GTPase (55).

PKD1 activation during pathological cardiac remodeling in rodents. Importantly, we have found that PKD1 is activated not only in cultured cardiac myocytes exposed to hypertrophic agonists but also in response to stress stimuli that trigger

TABLE 1. Echocardiographic characterization of PKD1 transgenic (PKD1-Tg) mice[a]

Characteristic	Results by type and age (*n*) of mouse							
	Wild type				PKD1-Tg			
	4 wk (4)	6 wk (4)	8 wk (3)	12 wk (3)	4 wk (8)	6 wk (6)	8 wk (6)	12 wk (3)
HR	707 ± 23	674 ± 7	694 ± 5	675 ± 4	639 ± 23	580 ± 12	598 ± 20	581 ± 41
Awths (mm)	1.71 ± 0.04	1.76 ± 0.03	1.81 ± 0.02	1.89 ± 0.04	1.44 ± 0.04	1.38 ± 0.03	1.19 ± 0.06	0.94 ± 0.04
Awthd (mm)	0.93 ± 0.04	0.90 ± 0.01	0.92 ± 0.01	0.99 ± 0.02	0.79 ± 0.02	0.80 ± 0.02	0.69 ± 0.03	0.42 ± 0.05
PWths (mm)	1.72 ± 0.05	1.92 ± 0.05	2,02 ± 0.01	1.99 ± 0.02	1.52 ± 0.02	1.49 ± 0.03	1.39 ± 0.02	1.37 ± 0.03
PWthd (mm)	0.93 ± 0.02	1.03 ± 0.04	1.01 ± 0.03	1.09 ± 0.02	0.82 ± 0.02	0.85 ± 0.03	0.74 ± 0.06	0.66 ± 0.04
LVIDs (mm)	0.41 ± 0.05	0.46 ± 0.04	0.43 ± 0.06	0.44 ± 0.01	1.81 ± 0.19	2.17 ± 0.19	2.62 ± 0.19	3.59 ± 0.44
LVIDd (mm)	2.27 ± 0.08	2.29 ± 0.04	2.39 ± 0.11	2.38 ± 0.02	3.03 ± 0.24	3.70 ± 0.23	4.00 ± 0.11	4.76 ± 0.27
% FS	81.8 ± 0.9	80.3 ± 0.9	81.1 ± 0.4	81.2 ± 0.4	44.0 ± 2.8	40.3 ± 2.3	34.4 ± 2.6	25.5 ± 4.0

[a] Data are expressed as means ± standard errors of the means. HR, heart rate; AWthd, anterior wall thickness in diastole; AWths, anterior wall in systole; PWthd, posterior wall thickness in diastole; PWths, posterior wall thickness in systole; LVIDd, left ventricular internal diameter in diastole; LVIDs, left ventricular internal diameter in systole; FS, left ventricular fractional shortening, calculated as (LVIDd − LVIDs)/LVIDd.

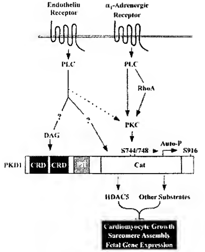

FIG. 9. A model for PKC-dependent and −independent activation of PKD1 in the control of cardiac hypertrophy. Cardiac hypertrophic agonists that signal via the α_1-AR or the ET-R stimulate PKC via PLC, resulting in PKC-directed phosphorylation of S744/748 in the activation loop of PKD1. In the case of the α_1-AR, PKC signaling is required for activation of PKD1. The ET-R is able to stimulate PKD1 catalytic activity in the absence of PKC signaling. PKC-independent activation of PKD1 may involve direct binding of the PLC product diacylglycerol (DAG) to the cysteine-rich domains (CRDs) of PKD1 or posttranslational modification of PKD1 at sites other than S744/748. The small GTPase RhoA, which lies downstream of several cardiac GPCRs, stimulates PKD1 in a PKC-dependent manner. PKD1 signaling contributes to cardiomyocyte growth, sarcomere assembly, and fetal gene activation through phosphorylation of the antihypertrophic protein HDAC5 and likely other substrates.

pathological cardiac hypertrophy in vivo. These results suggest a causal role for PKD1 signaling in the control of pathological cardiac growth. It will be of interest to determine the mechanism by which PKD1 is activated in vivo and whether or not this kinase is selectively stimulated in response to pathological stimuli, or if it also plays a role in physiological cardiac growth in response to exercise.

GPCR signaling to PKD1. Each of the agonists shown here to stimulate PKD1 in NRVMs functions via a GPCR that couples to the G_q alpha subunit of heterotrimeric G proteins. These results are consistent with numerous prior studies with nonmyocytes showing that GPCR agonists such as bombesin and vasopressin trigger activation of PKD (40). Surprisingly, we found that signaling via β-ARs, which are GPCRs that couple to G_s and G_i, does not activate PKD1 in vitro or in vivo. β-ARs are abundant in NRVMs and adult cardiac myocytes (33) and have been shown to play a key role in the control of cardiac remodeling (3). One downstream effector of β-AR signaling is protein kinase A (PKA), and a recent report by Carnegie et al. revealed the existence of a complex in adult rat heart containing PKD1, PKA, and the anchoring protein AKAP-Lbx (4). It will be of interest to elucidate the potential role of PKA-PKD1 interactions in the control of cardiac remodeling.

Subcellular distribution of PKD1 in cardiac myocytes. We propose that PKD1-directed phosphorylation of HDAC5 occurs in the nucleus. In this regard, prior studies have shown that PKD1, PKD2, and PKD3 exhibit the capacity to shuttle from the cytoplasm to the nucleus in response to agonists (2, 38, 39), and our immunofluorescence studies also revealed increased nuclear PKD1 in NRVMs treated with hypertrophic stimuli (Fig. 5B).

Our studies revealed prominent localization of PKD1 to perinuclear regions of cardiac myocytes in response to α_1-AR or ET-R signaling (Fig. 5B). The observed staining pattern may represent PKD1 associated with the *trans*-Golgi network. Indeed, prior studies have shown that PKD1 interacts with the *trans*-Golgi network via its CRDs and thereby regulates transport of proteins to the plasma membrane (25, 46).

In contrast to our findings, a recent report by Iwata et al. showed that PKD1 translocates to Z-disks of sarcomeres in NRVMs stimulated with agonists such as ET-1 (20). The reason for the differences between our findings and those of Iwata et al. are unknown. A role for PKD1 signaling at the level of the sarcomere was also suggested by Haworth et al., who demonstrated that PKD1 is capable of phosphorylating cardiac troponin I, a component of the sarcomere that inhibits actomyosin crossbridge cycling (17). However, it should be noted that cardiac troponin I is most abdundant in adult heart, and our studies were performed with neonatal cardiac myocytes.

Does PKD1 regulate other class II HDACs? The extent to which PKD1 signaling controls other class II HDACs is not currently known. However, the PKD-responsive serine residues in HDAC5 are conserved in HDACs 4, 7, and 9, and ectopic overexpression of PKD1 in fibroblasts is sufficient to drive HDAC4 and HDAC7 from the nucleus to the cytoplasm (5). In addition, PKD1 has been implicated in the regulation of HDAC7 nuclear export in activated T lymphocytes (37). HDAC4 has been shown to regulate chondrocyte hypertrophy (48), while HDAC7 appears to control endothelial cell adhesion (S. Chang and E. N. Olson, unpublished) and T-cell apoptosis (9). HDAC9 governs cardiac hypertrophy and was recently shown to control changes in skeletal muscle gene expression mediated by electrical stimulation (31). Thus, PKD1 signaling may elicit diverse biological effects via phosphorylation of class II HDACs.

Conclusions. Our findings suggest that small-molecule inhibitors of PKD1 may interrupt the terminal progression from cardiac insult to remodeling, heart failure, and death. A challenge for the future will be to develop selective antagonists of PKD1 for use in proof-of-concept studies with animal models of heart failure. In addition, it will be essential to assess the functional consequences of genetic deletion of PKD1 and/or PKD2 and PKD3 on the heart. In this regard, PKD isoforms have been implicated in many biological processes in diverse organ system, and thus it will likely be necessary to conditionally disrupt PKD genes selectively in the heart. Together, these chemical and genetic approaches promise to provide valuable new insight into the molecular underpinnings of pathological cardiac remodeling.

ACKNOWLEDGMENTS

We are grateful to D. Hood, C. Roberts, and K. Joly for excellent technical assistance, S. McCune for SHHF rats, N. Pagratis for advice regarding Cellomics imaging, S. Al-Murrani for advice on siRNA, and numerous members of Myogen R&D for input during the course of this work.

E.N.O. was supported by grants from the NIH, the Donald W. Reynolds Clinical Cardiovascular Research Center, the Robert A. Welch Foundation, and the Texas Advanced Technology Program.

REFERENCES

1. **Antos, C. L., T. A. McKinsey, M. Dreitz, L. M. Hollingsworth, C. L. Zhang, K. Schreiber, H. Rindt, R. J. Gorczynski, and E. N. Olson.** 2003. Dose-dependent blockade to cardiomyocyte hypertrophy by histone deacetylase inhibitors. J. Biol. Chem. **278:**28930–28937.
2. **Auer, A., B. J. von Blume, S. Sturany, W. G. von Wichert, L. J. Van Lint, J. Vandenheede, G. Adler, and T. Seufferlein.** 2005. Role of the regulatory domain of protein kinase D2 in phorbol ester binding, catalytic activity, and nucleocytoplasmic shuttling. Mol. Biol. Cell **16:**4375–4385.
3. **Bristow, M. R., N. E. Kantrowitz, R. Ginsburg, and M. B. Fowler.** 1985. Beta-adrenergic function in heart muscle disease and heart failure. J. Mol. Cell Cardiol. 17(Suppl. 2):41–52.
4. **Carnegie, G. K., F. D. Smith, G. McConnachie, L. K. Langeberg, and J. D. Scott.** 2004. AKAP-Lbc nucleates a protein kinase D activation scaffold. Mol. Cell 15:889–899.
5. **Chang, S., S. Bezprozvannaya, S. Li, and E. N. Olson.** 2005. An expression screen reveals modulators of class II histone deacetylase phosphorylation. Proc. Natl. Acad. Sci. USA **102:**8120–8125.
6. **Chang, S., T. A. McKinsey, C. L. Zhang, J. A. Richardson, J. A. Hill, and E. N. Olson.** 2004. Histone deacetylases 5 and 9 govern responsiveness of the heart to a subset of stress signals and play redundant roles in heart development. Mol. Cell. Biol. **24:**8467–8476.
7. **Chien, K. R.** 1999. Stress pathways and heart failure. Cell **98:**555–558.
8. **Chiu, T., and E. Rozengurt.** 2001. PKD in intestinal epithelial cells: rapid activation by phorbol esters, LPA, and angiotensin through PKC. Am. J. Physiol. Cell Physiol. **280:**C929–C942.
9. **Dequiedt, F., H. Kasler, W. Fischle, V. Kiermer, M. Weinstein, B. G. Herndier, and E. Verdin.** 2003. HDAC7, a thymus-specific class II histone deacetylase, regulates Nur77 transcription and TCR-mediated apoptosis. Immunity **18:**687–698.
10. **Devereux, R. B.** 1989. Importance of left ventricular mass as a predictor of cardiovascular morbidity in hypertension. Am. J. Hypertens. **2:**650–654.
11. **Dorn, G. W., and T. Force.** 2005. Protein kinase cascades in the regulation of cardiac hypertrophy. J. Clin. Investig. **115:**527–537.
12. **Frey, N., and E. N. Olson.** 2003. Cardiac hypertrophy: the good, the bad, and the ugly. Annu. Rev. Physiol. **65:**45–79.
13. **Gardin, J. M., and M. S. Lauer.** 2004. Left ventricular hypertrophy: the next treatable, silent killer? JAMA **292:**2396–2398.
14. **Grozinger, C. M., and S. L. Schreiber.** 2000. Regulation of histone deacetylase 4 and 5 and transcriptional activity by 14-3-3-dependent cellular localization. Proc. Natl. Acad. Sci. USA **97:**7835–7840.
15. **Gulick, J., A. Subramaniam, J. Neumann, and J. Robbins.** 1991. Isolation and characterization of the mouse cardiac myosin heavy chain genes. J. Biol. Chem. **266:**9180–9185.
16. **Harrison, B. C., C. R. Roberts, D. B. Hood, M. Sweeney, J. M. Gould, E. W. Bush, and T. A. McKinsey.** 2004. The CRM1 nuclear export receptor controls pathological cardiac gene expression. Mol. Cell. Biol. **24:**10636–10649.
17. **Haworth, R. S., F. Cuello, T. J. Herron, G. Franzen, J. C. Kentish, M. Gautel, and M. Avkiran.** 2004. Protein kinase D is a novel mediator of cardiac troponin I phosphorylation and regulates myofilament function. Circ. Res. 95:1091–1099.
18. **Haworth, R. S., M. W. Goss, E. Rozengurt, and M. Avkiran.** 2000. Expression and activity of protein kinase D/protein kinase C mu in myocardium: evidence for alpha1-adrenergic receptor- and protein kinase C-mediated regulation. J. Mol. Cell Cardiol. 32:1013–1023.
19. **Hilal-Dandan, R., C. K. Means, A. B. Gustafsson, M. R. Morissette, J. W. Adams, L. L. Brunton, and B. J. Heller.** 2004. Lysophosphatidic acid induces hypertrophy of neonatal cardiac myocytes via activation of Gi and Rho. J. Mol. Cell Cardiol. 36:481–493.
20. **Iwata, M., A. Maturana, M. Hoshijima, K. Tatematsu, T. Okajima, J. R. Vandenheede, L. J. Van, K. Tanizawa, and S. Kuroda.** 2005. PKCepsilon-PKD1 signaling complex at Z-discs plays a pivotal role in the cardiac hypertrophy induced by G-protein coupling receptor agonists. Biochem. Biophys. Res. Commun. 327:1105–1113.
21. **Kao, H. Y., A. Verdel, C. C. Tsai, C. Simon, H. Juguilon, and S. Khochbin.** 2001. Mechanism for nucleocytoplasmic shuttling of histone deacetylase 7. J. Biol. Chem. **276:**47496–47507.
22. **Kuo, M. H., and C. D. Allis.** 1998. Roles of histone acetyltransferases and deacetylases in gene regulation. Bioessays **20:**615–626.
23. **Lemonnier, J., C. Ghayor, J. Guicheux, and J. Caverzasio.** 2004. Protein kinase C-independent activation of protein kinase D is involved in BMP-2-induced activation of stress mitogen-activated protein kinases JNK and p38 and osteoblastic cell differentiation. J. Biol. Chem. **279:**259–264.
24. **Liao, J. K.** 2004. Statin therapy for cardiac hypertrophy and heart failure. J. Investig. Med. **52:**248–253.
25. **Maeda, Y., G. V. Beznoussenko, J. Van Lint, A. A. Mironov, and V. Malhotra.** 2001. Recruitment of protein kinase D to the trans-Golgi network via the first cysteine-rich domain. EMBO J. **20:**5982–5990.
26. **Marks, A. R.** 2003. A guide for the perplexed: towards an understanding of the molecular basis of heart failure. Circulation **107:**1456–1459.
27. **Matthews, S. A., E. Rozengurt, and D. Cantrell.** 1999. Characterization of serine 916 as an in vivo autophosphorylation site for protein kinase D/protein kinase Cmu. J. Biol. Chem. **274:**26543–26549.
28. **McKinsey, T. A., and E. N. Olson.** 2005. Toward transcriptional therapies for the failing heart: chemical screens to modulate genes. J. Clin. Investig. **115:**538–546.
29. **McKinsey, T. A., C. L. Zhang, J. Lu, and E. N. Olson.** 2000. Signal-dependent nuclear export of a histone deacetylase regulates muscle differentiation. Nature **408:**106–111.
30. **McKinsey, T. A., C. L. Zhang, and E. N. Olson.** 2000. Activation of the myocyte enhancer factor-2 transcription factor by calcium/calmodulin-dependent protein kinase-stimulated binding of 14-3-3 to histone deacetylase 5. Proc. Natl. Acad. Sci. USA **97:**14400–14405.
31. **Mejat, A., F. Ramond, R. Bassel-Duby, S. Khochbin, E. N. Olson, and L. Schaeffer.** 2005. Histone deacetylase 9 couples neuronal activity to muscle chromatin acetylation and gene expression. Nat. Neurosci. **8:**313–321.
32. **Molkentin, J. D., J. R. Lu, C. L. Antos, B. Markham, J. Richardson, J. Robbins, S. R. Grant, and E. N. Olson.** 1998. A calcineurin-dependent transcriptional pathway for cardiac hypertrophy. Cell **93:**215–228.
33. **Morisco, C., D. C. Zebrowski, D. E. Vatner, S. F. Vatner, and J. Sadoshima.** 2001. Beta-adrenergic cardiac hypertrophy is mediated primarily by the beta(1)-subtype in the rat heart. J. Mol. Cell Cardiol. **33:**561–573.
34. **Okin, P. M., R. B. Devereux, S. Jern, S. E. Kjeldsen, S. Julius, M. S. Nieminen, S. Snapinn, K. E. Harris, P. Aurup, J. M. Edelman, H. Wedel, L. H. Lindholm, and B. Dahlof.** 2004. Regression of electrocardiographic left ventricular hypertrophy during antihypertensive treatment and the prediction of major cardiovascular events. JAMA **292:**2343–2349.
35. **Olson, E. N., and M. D. Schneider.** 2003. Sizing up the heart: development redux in disease. Genes Dev. **17:**1937–1956.
36. **Onodera, T., T. Tamura, S. Said, S. A. McCune, and A. M. Gerdes.** 1998. Maladaptive remodeling of cardiac myocyte shape begins long before failure in hypertension. Hypertension **32:**753–757.
37. **Parra, M., H. Kasler, T. A. McKinsey, E. N. Olson, and E. Verdin.** 2005. Protein kinase D1 phosphorylates HDAC7 and induces its nuclear export after T-cell receptor activation. J. Biol. Chem. **280:**13762–13770.
38. **Rey, O., J. Sinnett-Smith, E. Zhukova, and E. Rozengurt.** 2001. Regulated nucleocytoplasmic transport of protein kinase D in response to G protein-coupled receptor activation. J. Biol. Chem. **276:**49228–49235.
39. **Rey, O., J. Yuan, S. H. Young, and E. Rozengurt.** 2003. Protein kinase C nu/protein kinase D3 nuclear localization, catalytic activation, and intracellular redistribution in response to G protein-coupled receptor agonists. J. Biol. Chem. **278:**23773–23785.
40. **Rozengurt, E., O. Rey, and R. T. Waldron.** 2005. Protein kinase D signaling. J. Biol. Chem. **280:**13205–13208.
41. **Storz, P., H. Doppler, F. J. Johannes, and A. Toker.** 2003. Tyrosine phosphorylation of protein kinase D in the pleckstrin homology domain leads to activation. J. Biol. Chem. **278:**17969–17976.
42. **Storz, P., and A. Toker.** 2003. Protein kinase D mediates a stress-induced NF-kappaB activation and survival pathway. EMBO J. **22:**109–120.
43. **Sugden, P. H.** 2001. Signalling pathways in cardiac myocyte hypertrophy. Ann. Med. 33:611–622.
44. **Sugden, P. H.** 2003. An overview of endothelin signaling in the cardiac myocyte. J. Mol. Cell Cardiol. 35:871–886.
45. **Vakili, B. A., P. M. Okin, and R. B. Devereux.** 2001. Prognostic implications of left ventricular hypertrophy. Am. Heart J. 141:334–341.
46. **Van Lint, J., A. Rykx, Y. Maeda, T. Vantus, S. Sturany, V. Malhotra, J. R. Vandenheede, and T. Seufferlein.** 2002. Protein kinase D: an intracellular traffic regulator on the move. Trends Cell Biol. 12:193–200.
47. **Vega, R. B., B. C. Harrison, E. Meadows, C. R. Roberts, P. J. Papst, E. N. Olson, and T. A. McKinsey.** 2004. Protein kinases C and D mediate agonist-dependent cardiac hypertrophy through nuclear export of histone deacetylase 5. Mol. Cell. Biol. **24:**8374–8385.
48. **Vega, R. B., K. Matsuda, J. Oh, A. C. Barbosa, X. Yang, E. Meadows, J. McAnally, C. Pomajzl, J. M. Shelton, J. A. Richardson, G. Karsenty, and E. N. Olson.** 2004. Histone deacetylase 4 controls chondrocyte hypertrophy during skeletogenesis. Cell 119:555–566.
49. **Verdin, E., F. Dequiedt, and H. G. Kasler.** 2003. Class II histone deacetylases: versatile regulators. Trends Genet. 19:286–293.
50. **Waldron, R. T., O. Rey, T. Iglesias, T. Tugal, D. Cantrell, and E. Rozengurt.** 2001. Activation loop Ser744 and Ser748 in protein kinase D are transphosphorylated in vivo. J. Biol. Chem. **276:**32606–32615.
51. **Waldron, R. T., O. Rey, E. Zhukova, and E. Rozengurt.** 2004. Oxidative stress induces protein kinase C-mediated activation loop phosphorylation and nuclear redistribution of protein kinase D. J. Biol. Chem. **279:**27482–27493.
52. **Waldron, R. T., and E. Rozengurt.** 2003. Protein kinase C phosphorylates protein kinase D activation loop Ser744 and Ser748 and releases autoinhibition by the pleckstrin homology domain. J. Biol. Chem. **278:**154–163.
53. **Wood, C. D., U. Marklund, and D. A. Cantrell.** 2005. Dual phospholipase C/diacylglycerol requirement for protein kinase D1 activation in lymphocytes. J. Biol. Chem. **280:**6245–6251.

54. **Yang, X. J., and S. Gregoire.** 2005. Class II histone deacetylases: from sequence to function, regulation, and clinical implication. Mol. Cell. Biol. **25:**2873–2884.
55. **Yuan, J., L. W. Slice, and E. Rozengurt.** 2001. Activation of protein kinase D by signaling through Rho and the alpha subunit of the heterotrimeric G protein G13. J. Biol. Chem. **276:**38619–38627.
56. **Zhang, C. L., T. A. McKinsey, S. Chang, C. L. Antos, J. A. Hill, and E. N. Olson.** 2002. Class II histone deacetylases act as signal-responsive repressors of cardiac hypertrophy. Cell **110:**479–488.
57. **Zhang, W., R. C. Kowal, F. Rusnak, R. A. Sikkink, E. N. Olson, and R. G. Victor.** 1999. Failure of calcineurin inhibitors to prevent pressure-overload left ventricular hypertrophy in rats. Circ. Res. **84:**722–728.
58. **Zugaza, J. L., R. T. Waldron, J. Sinnett-Smith, and E. Rozengurt.** 1997. Bombesin, vasopressin, endothelin, bradykinin, and platelet-derived growth factor rapidly activate protein kinase D through a protein kinase C-dependent signal transduction pathway. J. Biol. Chem. **272:**23952–23960.